10th World Congress on Structural and Multidisciplinary Optimization
May 19 - 24, 2013, Orlando, Florida, USA

Wing Topology Optimization with Self-Weight Loading

Luís Félix[1], Alexandra A. Gomes[2], Afzal Suleman[3]

[1]Portuguese Air Force Academy, Sintra, Portugal, lffelix@academiafa.edu.pt
[2]IDMEC, Instituto Superior Técnico, Technical University of Lisbon, Lisbon, Portugal, magoncal@dem.ist.utl.pt
[3]University of Victoria, Dept. of Mechanical Engineering, Victoria, BC, V8W 2Y2 Canada, suleman@uvic.ca

1. Abstract
In this work is presented a material model to include self-weight loads in topology optimization. The proposed approach is focused in the optimization of lifting structures and aims not only to eliminate numerical instabilities due to the weight load, but also to improve the solution quality. The algorithm is tested in a two-dimensional benchmark for validation purposes. The loading of the domain resembles a lifting structure's one and two methods are employed to solve the problem: a single load formulation that results in a very stiff structure for the design load, but performs poorly in a rest situation (only weight load present); and a multiple load formulation that converges to a balanced solution. Results of this problem shows that the method implemented improves the discreteness of the design of structures subjected to load cases similar to lifting structures.
After validation, it is optimized the full interior body of a wing where the skin is left out of the design domain. The aerodynamic load is computed assuming a rigid wing body, and the loading condition is completed with the structure self-weight. In a first approach, the aerodynamic load is much larger than the wing weight, simulating an airliner wing and the results shows the merits of the code implemented. Then, the wing is optimized assuming an aerodynamic load matching the wing weight in order to simulate a flying wing aircraft configuration.
2. Keywords: Topology Optimization, SIMP-like approach, wing design, self-weight load.

3. Introduction
The classical approach to topology optimization of structural boundaries is homogenization and was first introduced by Bendsøe and Kikuchi [1] in the late eighties. Since then, other methods have been proposed and researched. In this work is adopted the method proposed by Rozvany and Zhou [2], specially developed for large scale problems, called SIMP.

Although topology optimization of continuum structures is a recent technique, it found its way to industry extremely rapidly, aircraft design being no exception to that. Despite the successes in the automotive industry, topology optimization has not yet become a mainstream for the design of aircraft components. This is partly due to larger problem sizes and more complicated support and loading conditions for aircraft components. Additionally, compliance minimization is the most solved and researched topology optimization problem, and compliance based methods stills lacks the ability to deal with buckling criteria, a major requirement for aircraft components. One of the few examples of aircraft with components designed with topology optimization is the A380 [3]. Airbus UK and Altair used topology optimization methods, based on the SIMP approach, to redesign the inboard inner and outer fixed leading edge ribs and to redesign the fuselage door intercostals of the A380 with weight savings in the order of 1000 kg per aircraft.

Other examples of application of SIMP-like methods for aerospace design are the work of Maute and Reich [4], and Gaspari and Ricci [5]. Maute and Reich have used a similar approach to the SIMP method in a framework tool for design of mechanisms in morphing airfoils. The method proposed merges topology optimization with aeroelastic design optimization, and it is used to design a morphing airfoil section to maximize lift-to-drag ratio, whereas applying aerodynamic and structural constraints. Gaspari and Ricci have also developed a strategy to design morphing airfoils that combines aerodynamic and structural optimization where they apply topology optimization. The aim is to determine the most efficient aerodynamic shape while minimizing the necessary energy to change the airfoil shape.

There are also some examples of the application of level set methods to aircraft design. Gomes and Suleman [6] have used a spectral level set method to design a reinforced wing box to enhance roll manoeuvrability which can be attained by maximizing aileron reversal speed. Topology optimization is used to reinforce the upper skin of the wing torsion box. James and Martins [7] used a isoparametric

level set method to optimize a three dimensional wingbox body subject to a fixed approximation of the aerodynamic load.

In a previous work, we have already used topology optimization to minimize the compliance of a wing with an aerodynamic load applied (see ref. [8]). In this paper we address the compliance minimization problem of a full three-dimensional wing while subjected both to aerodynamic loads and its self-weight load. We propose a new material model that, not only overcomes the numerical instabilities associated with the density dependent loads (see ref. [9]), but it also improves the solution quality when used to design lifting structures or any other structure with a similar loading.

4. Compliance Minimization Using SIMP Method

The minimum compliance problem objective is to find the optimal material distribution of a body (structure, mechanical element, etc.) within a given domain Ω that minimizes the deformation of the body for the applied loads and boundary conditions. In other words, the objective is to maximize the structure stiffness. In a finite element model, the minimum compliance problem with a material volume constraint is stated as [10]

$$\begin{aligned} \text{minimize} \quad & c(\boldsymbol{\mu}) = \mathbf{F}^T\mathbf{u} \\ \text{Subjected to:} \quad & \sum_{e=1}^{N} v_e\mu_e \leq V \\ & \mathbf{K}\mathbf{u} - \mathbf{F} = 0 \\ & 0 \leq \mu_e \leq 1 \qquad e = 1, \ldots, N \end{aligned} \tag{1}$$

where c is the compliance of the structure which can be written either as the work done by the external forces or as twice the total elastic energy at equilibrium, and is dependent of a non-physical variable that represents material density, μ. This variable is bounded between 0 and 1 and is used to represent the material properties, which, by introducing this variable, is assumed to have isotropic properties at macro-scale. Whereas the variable bounds represent void and solid phase, respectively, intermediate values of the variable identifies a non feasible material that shall be avoided. This non-physical variable can be assumed as the material density and, from now on, shall be referred to as pseudo-density. $\mathbf{F}$ is the external force vector and includes both body loads and surface loads, and $\mathbf{u}$ is the displacement field of the domain Ω at equilibrium. The element volume is represented by v_e and V is the maximum volume allowed within the domain of the problem. Besides the volume constraint, the structure must also satisfy the governing equation where $\mathbf{K}$ represents the global stiffness matrix.

Using the pseudo-density variable to represent the material properties over the domain, the effective material stiffness, E_e, of a given finite element or cell (a set of finite elements that share one common pseudo-density variable) can be expressed as the product of the material's Young's modulus, E_0, and an interpolating function of the element pseudo-density, μ_e,

$$E_e = \phi(\mu_e) E_0 \tag{2}$$

The function ϕ is a key aspect of the SIMP method since it is responsible to force the pseudo-density of each cell toward solid or void phase in the final solution. This is achieved by penalizing intermediate values of the variable. The most commonly used penalization function, and also the simplest, is the one proposed by Bendsøe[1], which is given by

$$\phi(\mu_e) = {\mu_e}^p \tag{3}$$

where the penalization parameter, p is some number greater than 1. When implemented with a volume constraint, this function penalizes intermediate density elements with reduced stiffness for a given mass.

In order to solve the optimization problem is necessary to solve a finite element analysis to compute the displacement field, u, in each iteration, which depends on the pseudo-density set representative of the design point. Since material properties depends on the element density, the global stiffness matrix of the structure must be computed based on the element pseudo-densities as follows,

$$\mathbf{K} = \sum_e \mathbf{k}_e(\mu_e) \tag{4}$$

Introducing the SIMP penalization function, the element stiffness matrix, $\mathbf{k}_e$, is itself a function of μ_e

$$\mathbf{k}_e = \phi(\mu_e)\, \mathbf{k}_{e_0} \tag{5}$$

where $\mathbf{k}_{e_0}$ is the stiffness matrix of the solid element ($\mu_e = 1$). Using the power law previously mentioned (Eq. (3)) as penalization function, the lower bound of μ_e defined in Eq. (1) must be redefined as higher than zero ($\mu_e \geq \mu_{min} > 0$), in order to avoid singularities in the global stiffness matrix. This way, the minimum element stiffness allowed in the problem is dependent of the penalization factor, p. Sigmund[11] proposed another interpolation function that allows to set the lower bound as zero and defines a minimum element stiffness, E_{min} independent of p. This function is stated as

$$\phi(\mu_e) = \eta + {\mu_e}^p (1 - \eta) \tag{6}$$

where η represents the ratio between the defined E_{min} and E_0. This function behaviour is similar to the power law proposed by Bendsøe. However, for $\mu = 0$ the penalization function is not zero and there is no need to set a lower bound μ_{min}. Moreover, at the lower bound of μ, which in this case is zero, it assumes a constant value, whereas the power law function depends not only of μ_{min} but also of p. This stiffness updating scheme is also more stable than the power law function when combined with a continuation method applied to parameter p.

Being the elimination of intermediate density elements a major concern in SIMP-like methods, it is interesting to have a measurement of the presence of these type of elements in the optimal solution. Such a parameter to measure the quantity of non-discrete elements is proposed by Sigmund [11] as,

$$M_{nd} = \frac{\sum_{e=1}^{N} 4\mu_e (1 - \mu_e)}{N} \times 100\% \tag{7}$$

When all intermediate density elements are eliminated from the solution, the above equation returns 0%, representing a very good solution. On the other hand, if all elements from the design domain present a pseudo-density of 0.5, the parameter becomes 100%, representing the worst case scenario. This parameter is very useful when used to compare the quality of solutions obtained for the same problem (with the same volume constraint) with different parameters, like the penalization factor or different regularization methods. However, it shall not be used to compare the solution quality between different problems, in particularly if the volume constraint is different. For example, consider the optimization of a structure with a volume constraint of 50% and 10%, respectively. An admissible structure, in terms of the volume constraint, would be an uniform distribution of material over the design domain, represented by a constant value of the pseudo-density set of 0.5 and 0.1, respectively. In the first case, the measurement of non-discreteness of the solution is 100%, whereas, with a volume constraint of 10%, the uniform material distribution returns a non-discreteness measurement of 36%. For this problem, 36% is also the maximum value allowed for this measurement assuming that the volume constraint is satisfied.

Material density based formulations to solve topology optimization problems, particularly when combined with penalizations functions, are prone to numerical instabilities [12, 13, 10]. The three main numerical challenges present in SIMP-like methods are mesh-dependency, checkerboard patterns and local minima. To deal with the first two type of instabilities it is used the well-known sensitivity filter suggested by Bendsøe and Sigmund [10] and three morphological based density filters (*combi*, *open*, and *close*) proposed by Sigmund [11]. Local minima problems are handled with the continuation method with different increment policies in function of the type of filter used. When using the sensitivity filter, parameter p is incremented 0.5 every 10 iterations or after convergence until it reach the maximum value of 6. If we select any of the morphological based filters, every 30 iterations or after convergence parameter p is increment 0,5 and parameter β (this parameter is introduced by this family of filters) is doubled until reaching the maximum values of 6 and 200, respectively.

Due to the number of design variables involved (there is one variable for each finite element) we use the Globally Convergent version of the Method of Moving Asymptotes (GCMMA)[14], which is an algorithm well suited to deal with many design variables and few constraints and has been used in a wide range of applications. To check problem convergence we have implemented two criteria that can be used independently or simultaneous. In the first one we calculate the iteration relative error and assume that the problem is converged if this error is lower than a value defined by the user. The other method obtains the design variables maximum change between two iterations and checks if this value is lower than the defined tolerance. When both methods are active, the first to satisfy all conditions determines problem convergence and we can check in the output file which criteria was fulfilled.

4.1. Self-Weight Load

Self-weight loads are dependent of the gravitational acceleration and material properties, in particular of the material density. Since that in material density based topology optimization formulations, like the SIMP method, the material properties are dependent of the design variable pseudo-density $\boldsymbol{\mu}$, self weight loads are also dependent of the design variable set. Usually, the element density ρ_e is related to the base material density ρ_0 as

$$\rho_e = \mu_e \rho_0 \tag{8}$$

Using this equation and the finite element shape functions it is possible to compute and apply the body load on the elements nodes. One of the major advantages of this method is that the self-weight load, in any step of the optimization problem, is directly proportional to the amount of material employed in the structure, whereas, for example, the structure stiffness is affected by the penalization function. Since the optimal solution is already driven toward a 0-1 design by penalizing the stiffness of intermediate density elements, there is no need to include an additional penalization in the relation between the element self-weight load and its pseudo-density. This way, the body load vector over the course of the optimization problem is truly representative of the material distribution on the design space. However, the different handling of the element density and stiffness in function of the design variable, can lead to local numerical instabilities at the FEM solver. From Eq. (8) the body load vector $\mathbf{b}$ is proportional to $\boldsymbol{\mu}$ and, when using the original power law (Eq. (3)) the global stiffness matrix is proportional to $\boldsymbol{\mu}^p$. Therefore the ratio between the structure weight and its stiffness becomes infinity when the pseudo-density tends to zero. Consequently, the displacement field and structure compliance become unbounded in the vicinity of the lower bound of the pseudo-density. For example, in a problem with a penalization factor of 3, if four elements share the same node and their pseudo-density μ is 0.01, the stiffness of the set will tend to E_{min} but the self-weight load on that node could still be significantly high. As a result, the displacement of that node, as also its contribution to the structure compliance, may become to large.

Most approaches to solve this problem focus on the element stiffness update function without changing the element density model. In this work is proposed a different approach where the original power law proposed by Bendsøe to drive the problem to a 0-1 solution is applied to the element density update model. The idea is to multiply the base material properties, ρ_0 and E_0, by equivalent coefficients for any value of the pseudo-density variable. However, since there is no need to assure a element density different from zero for numerical analysis, the element density is updated with the power law, instead of the penalization function of Eq. (6), due to its simplicity. Therefore, in this approach the element density is computed as

$$\rho_e = {\mu_e}^p \rho_0 \tag{9}$$

and the ratio between weight load and stiffness is constant, except in the vicinity of the lower bound of μ where ρ_e tends to zero whereas E_0 tends to ηE_0. Figure 1 plots the ratio between the weight load and stiffness obtained with $p = 3$ and $\eta = 10^{-6}$. The material model proposed suggest that, for most type of problems, the penalization of intermediate density elements is reduced, because an intermediate element presents a lower weight load per unit of volume. Therefore, in problems where the main load applied is the self-weight, a design with more gray elements has an effective lower load applied which may proof beneficial in terms of the structure compliance. However, the objective is to use this algorithm to optimize aircraft structures, specially lifting structures, where the main load is the lift force. In this type of problem, as the self-weight load increases, the total force applied on the structure reduces and, consequently, the compliance is also reduced. This way, for structures with lifting loads or similar ones, the proposed material model provides a stronger incentive to drive the solution towards a 0-1 design.

4.2. Sensitivity Analysis

Due to its formulation, a topology optimization problem includes several design variables, particularly when using the SIMP method where a design variable is assigned to each element belonging to the design space. Therefore, normally is used gradient-based methods for solving the optimization problem. The high dimensionality of the problem also requires an efficient analytical approach to compute the sensitivities. The most effective method to compute the derivatives is to use the adjoint method that avoids to compute the displacement sensitivities [10]. For the minimum compliance problem, it is possible to rewrite the objective function as

$$c\left(\rho\right) = \mathbf{F}^T\mathbf{u} - \tilde{\mathbf{u}}^T\left(\mathbf{K}\mathbf{u} - \mathbf{F}\right) \tag{10}$$

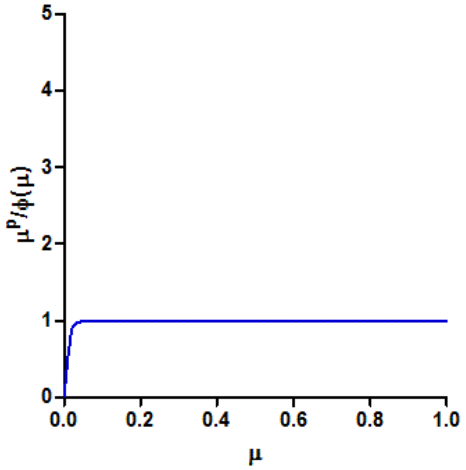

Figure 1: Weight load to stiffness ratio with proposed material model.

where $\tilde{\mathbf{u}}^T$ is any arbitrary fixed real vector. When $\tilde{\mathbf{u}}$ satisfies the adjoint equation $\mathbf{F}^T - \tilde{\mathbf{u}}^T\mathbf{K} = 0$, which for compliance implies that $\tilde{\mathbf{u}} = \mathbf{u}$, the derivative of the previous equation in order to the design variable $\boldsymbol{\mu}$ becomes

$$\frac{\partial c}{\partial \boldsymbol{\mu}} = 2\mathbf{u}^T \frac{\partial \mathbf{F}}{\partial \boldsymbol{\mu}} - \mathbf{u}^T \frac{\partial \mathbf{K}}{\partial \boldsymbol{\mu}} \mathbf{u} \tag{11}$$

If self-weight is neglected, the first term on the right of Eq. (11) vanishes and the derivative is always negative. This means that the objective function compliance is monotonous and one can use optimality conditions to build efficient strategies to solve the problem [10]. On the other hand, when body loads are considered we have to include the first term and the objective function can have a non-monotonous behaviour regarding the design variable μ_e [9].

Due to the form of the global stiffness matrix (Eq. (4)) and the element stiffness update scheme (Eq. (5)), one can compute the derivative of the stiffness term (second derivative in Eq. (11)) with respect to μ_e as

$$\frac{\partial c}{\partial \mu_e} = -{\mathbf{u}_e}^T \frac{\partial \mathbf{K}}{\partial \mu_e} \mathbf{u}_e = -p{\mu_e}^{p-1} (1-\eta) \, {\mathbf{u}_e}^T \mathbf{k}_{e_0} \mathbf{u}_e \tag{12}$$

where $\mathbf{u}_e$ represents the portion of the global displacement vector corresponding to the nodes of element e.

Assuming that there is a self-weight load it is necessary to compute the first term in Eq. (11). If there is access to the element body load vector we can easily obtain this derivative as

$$2{\mathbf{u}_e}^T \frac{\partial \mathbf{F}}{\partial \mu_e} = p{\mu_e}^{p-1} \mathbf{b}_{e_0} \tag{13}$$

where $\mathbf{b}_{e_0}$ represents the element body load vector with the base material density. Using these two equations, once the state of the system has been obtained by solving the governing equations, the sensitivities are directly computed.

5. Two-dimensional example

The algorithm discussed in this work is applied to design a two-dimensional cantilever beam that is subjected to a vertical, upward point force at the beam tip and its self-weight. This loading condition is similar to a wing in levelled flight, since the structure weight may be seen as a secondary load that counteracts the aerodynamic lift. The objective is to find a design with only 40% of material of the initial domain that minimizes the beam compliance. The design domain dimensions are 2 x 1 meter and it is modelled with a regular mesh of 80 x 40 four node elements with two degrees of freedom per node. The mechanical properties of the base material to be distributed in the domain are $E_0 = 1$ N/m^2 and $\nu = 0.3$ whereas the specific mass ρ_0 is 1.25 kg/m^3 and the point load is 1 N.

The results displayed in table 1 are obtained with the sensitivity and *combi* filters, and a filter radius $R_{filter} = 0.06$ m. As a reference, the problem is also solved without the self-weight load. In both simulations, parameters p and β (if necessary), are gradually incremented over the course of the optimization process as explained in section 4. As expected the compliance of the structure decreases when the weight load is considered. The numerical results also show that the non-discreteness measurement, of both solutions, decreases as the weight load is applied. This tendency, also verified in the wing design problem (see section 6), effectively prove that the proposed material model not only solves the problem of unbounded displacements but it also forces the solution towards a 0-1 design. The optimum solution topology obtained with the sensitivity filter is portrayed in figure 2(a). With the considered load case, the tendency is to move the material toward the free edge so that the bending moment due to body load minimizes the resulting bending moment due to the point load. It is observable that most of the material is placed near the free edge.

Table 1: Cantilever beam optimization results.

	Sensitivity filter		*Combi* filter	
	$f(x)$	M_{nd} [%]	$f(x)$	M_{nd} [%]
no self-weight	93.17	7.69	91.55	2.01
$\rho_0 = 1.25$ kg/m^3	31.10	5.22	33.45	1.16

The optimum structure obtained with the sensitivity filter is evaluated again with and without the point force, and the penalization of intermediate density elements is removed. The results are presented in table 2. By comparison with table 1, one may conclude that the weight load increases when the penalization law is removed. Without penalization, the compliance of the structure is lower than the optimum solution obtained with penalization. This is expected since the material model employed not only penalizes the stiffness of intermediate density elements, as it also reduces their specific weight. Since in this example the point force and the weight load are applied in opposite directions, the compliance decreases as the structure weight increases.

When the structure is subjected to the weight load only, i.e., when it is in rest, its compliance is very large. Indeed, the structure deformation is higher while in rest than when it is loaded with the point force. The compliance of this structure while subjected only to its self-weight is even higher than the compliance of the beam optimized to support the point force without considering the self-weight load (the compliance value of this design with non-penalized intermediate density elements is 83.96 instead of the value presented in table 1). It must be mentioned that the point force and the self-weight load have the same magnitude, but whereas the point force is concentrated in the farthest point from the beam support, the self-weight load is distributed over the structure domain. Thus, the single point force is more demanding than the distributed self-weight load.

Table 2: Compliance of sensitivity filter solution in different loading conditions.

	Single load formulation	Multi load formulation
Full load case	27.03	37.5
Only weight load	91.05	18.32

In order to obtain a design that performs well in both situations, the problem may be solved with a multiple load formulation. In this example the objective function is defined as the sum of the structure compliance values, with equal weights, for two different loads cases: the full load case, and only the self-weight load. The gravitational acceleration load is always present because it would not have physical meaning to optimize the structure to a point force without the weight load when it is assumed that gravitational load has a major role in the structure design and behaviour.

In figure 2(b) is plotted the multiple load formulation design obtained with the sensitivity filter. The design is much more balanced than the solution derived from the single load formulation including self-weight load. It is also placed an extra amount of material near the beam edge in order to increase the

weight bending moment, but must of the material is used to reinforce the beam in the vicinity of it's fixing point. As shown in figure 2(a), the single load formulation problem results in a design with a much higher concentration of material on the free edge. Although this design presents a lower compliance for the complete load case, it is very penalized when is considered only the self-weight load. Therefore, the solution must be a compromise between using the weight to reduce the beam displacement while the point force is applied and the deformation due to the material distribution in a situation without the point force.

(a) Single load formulation. (b) Multi load formulation.

Figure 2: Cantilever beam optimum design obtained with the sensitivity filter in (a) single load and (b) multiple load formulations.

The compliance of the optimum design obtained with the sensitivity filter was evaluated without penalization of intermediate density element, while subjected to the two load cases identified. The results are displayed in table 2 and show that the behaviour of this solution is quite different from the previous design obtained with the single load formulation, which results are plotted in the same table. On the one hand, this structure's deformation is slightly larger when submitted to the complete load case, since it has a higher compliance. On the other hand, the displacement due to the self-weight load is drastically reduced. In this case, the deformation of the beam in rest (i.e., without the point force applied) is lower than when it must support the point force, as it is expected for any structure.

In this example, the objective function is the direct sum of the compliance of the load cases, where the weights of each compliance are set to 1. However, it is possible to assign different weights to each load case in order to give more preponderance in the design to a specific loading condition. For example, if a higher weight is assigned to the complete load case, the design obtain will be more closer to the structure represented in figure 2(a), whereas if the weight of the self-weight load case is higher, the solution is driven towards a design obtained for a no self-weight load solution.

6. Application to wing optimization

In this section the algorithm implemented is used to optimize the material distribution among the interior volume of a wing. The objective is to maximize the wing stiffness with a maximum material volume of 10% of the wing core. Besides the self-weight load the wing is subject to the aerodynamic load equivalent to a level flight at Mach 0.7 at an altitude of 11000 meters and an angle of attack of 4 degrees, which is computed with a panel method code assuming a rigid body. This means that the aerodynamic load is computed in a pre-processing step and is assumed constant over the course of the problem.

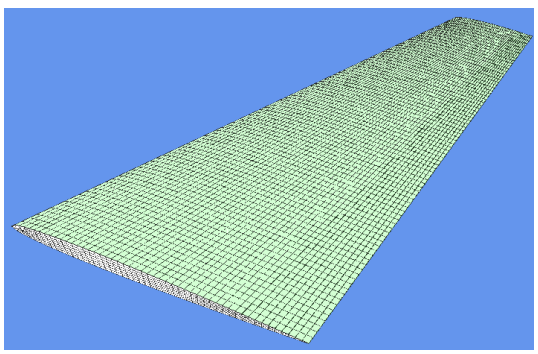

Figure 3: Wing design domain.

The design space is defined by a wing with a semi-span of 10 meters and a leading edge sweep of 32.25 degrees, whereas the the airfoil section is a NACA 0010. The wing model is represented in figure 3, and is modelled by a total of 29797 elements, from which 21497 are design variables. The wing skin is defined with 4 nodes shell elements which are not included in the design variable set. Since the aerodynamic load is applied directly on the skin elements, it is not pseudo-density dependent. The base material of the wing is an aluminium alloy with the following properties: $E_0 = 70$ Gpa, $\nu = 0.33$, and $\rho_0 = 2400$ kg/m^3. As mentioned before, the aerodynamic load is applied directly on the skin which has a thickness of 2.5 mm and all degrees of freedom at the wing root are fixed. The optimization problem is solved with the four filters implemented, the sensitivity filter and the three morphological based density filters, which have an area of influence defined by $R_{filter} = 0.15$ m. In order to try to overcome the problem of local minima, both parameters p and β (if necessary), are gradually incremented over the course of the optimization process as explained in section 4.

Table 3: Wing optimum design compliance and non-discreteness measurement.

	Sensitivity filter		*Close* filter		*Open* filter		*Combi* filter	
	$f(x)$	M_{nd} [%]	$f(x)$	M_{nd} [%]	$f(x)$	M_{nd} [%]	$f(x)$	M_{nd} [%]
no self-weight	2635.76	8.20	3141.09	0.89	3587.33	6.26	3488.83	3.86
$\rho_0 = 2400$ kg/m^3	2228.66	7.54	2527.47	0.84	3008.03	5.57	2905.73	3.75

The results obtained in the different simulations, which are distinguish by the filter technique active, are presented in Table 3. As a reference, is also presented data from previous results obtained without self-weight load [8]. As expected, the optimum compliance decreases when we apply the self-weight load. But more important is the tendency revealed in the non-discreteness measurement. Even though, the difference is small, in all runs executed, the problem with self-weight load converges to a solution with better quality, i.e., with less gray elements. These results shows that the tendency already observable in the two-dimensional benchmark problem is also verified in a three-dimensional design domain and modelled with a non-uniform mesh as in this case.

The optimum design obtained with the *combi* filter is plotted in figure 4. Again, the no weight load solution is used as a comparison reference. The plotted results shows that the structure shape does not alter significantly, despite the reduction in the compliance achieved. This means that the lower deformation energy is obtained mostly due to the self-weight load action and not from a different distribution of the material. As the wing self-weight load is much lower than the lift force, it does not compensate to dislocate material to the wing tip. The reduction in bending moment that one would achieve is not enough to counterbalance the lower stiffness of the structure near the root.

In this example the lifting load is much greater than the weight load, like in a conventional airliner's wing. In order to test the algorithm in a situation were the weight load has more influence in the design process, the problem was reformulated with a lower aerodynamic load, equivalent to a flying wing configuration. The aerodynamic load is obtained from a level flight condition at Mach 0.52, 2 degrees of angle of attack and 11000 meters of altitude. The optimum design obtained with the *combi* filter is plotted in figure 5(a). In this case, since the lifting and weight load have matching magnitudes, the optimum structure topology reflects the influence of weight load that results in the placement of more material near the wing tip.

Although the structure plotted in figure 5(a) may be optimal for a flight cruise condition, most probably it will succumb in a stationary situation with no aerodynamic load or in flight with high g's loads, because the structure is too weakened near the root. A better approach for this problem is to consider a multiple load formulation where, besides the flight cruise condition, is considered an high g-manoeuvre.

The wing design problem was solved again with a multiple load formulation, assuming two flight situations: levelled flight and a 3-g manoeuvre. In this simulation, is assigned an equal weight in the objective function for both loading conditions. The optimum wing's structure design is portrayed in figure 5(b), which shows that the solution is completely different form the previous one obtained with the single load formulation. Indeed, the solution obtained is very similar to the airliner's design plotted in figure 4(b). The difference between these two designs resides in the main spar length that is slightly greater in the last example.

In table 4 is compared the non-penalized compliance of the four designs obtained (see figures 4 and 5)

due to two aerodynamic loads, equivalent to the 1-g and 3-g flight of the flying wing. The data collected show us that the influence of the weight load in the wing's design is very small when high g's loads are assumed. Not only the structure's designs associated to the last three columns are identical, but also the non-penalized compliance is very similar for both load cases considered. Since the last one was obtained without considering the weight load in the optimization process, these results proves that the material weight is not a driving parameter in wing's design, when different flight conditions are taken into account. The data presented also suggest that for wing's structure design, one may leave out the 1-g load condition. Although the design obtained with the multiple load formulation presents a better overall performance, the airliner's wing has a very similar behaviour in both loading conditions assumed.

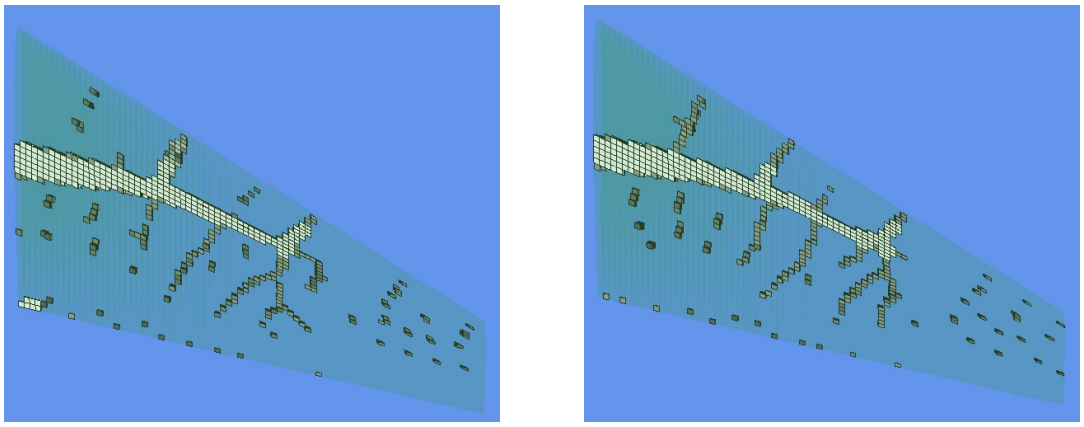

(a) No self-weight load.

(b) $\rho_0 = 2400$ kg/m^3.

Figure 4: Wing optimum design obtained with *combi* filter.

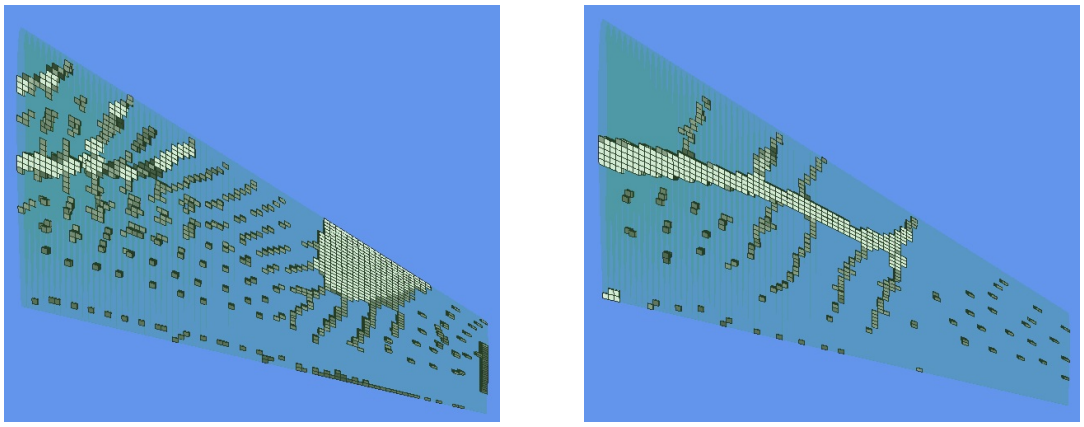

(a) Single load formulation.

(b) Multiple load formulation.

Figure 5: Flying wing optimum designs obtained with *combi* filter in (a) single load and (b) multiple load formulations.

Table 4: Non penalized compliance values for two flight conditions (1-g and 3-g flight) and four wing designs: the single load formulation solutions of the flying wing and the airliner's wing; the multiple load formulation design; and the design obtained without weight load.

	Flying wing	Airliner's wing	Multiple load design	no weight load design
1-g flight	19.95	50.54	45.59	55.49
3-g flight	1134.8	896.03	888.09	943.48

7. Conclusion

We have presented an approach to structural topology optimization applied to full three-dimensional domains and taking into account the structure self-weight. The algorithm was applied to a two-dimensional problem that validate our material model for topology optimization regarding the self-weigh load. Validation tests also allowed to prove that the method used to update the element density increases the solution discreteness quality in the particular case of optimization of structures with load cases similar to a lifting surface.

Practical application is given to the topology optimization tool in the form of wing design problems. First, it is optimized an airliner's wing, where the lift force is much greater than the structure self-weight load. Then a flying wing configuration is optimized. Due to the results obtained, the last simulation was resolved with a multiple load formulation that considers two flight conditions: levelled flight and a 3-g flight. A comparative study of the non-penalized compliance of the four designs obtained shows that the influence of weight loads in wing's design is very small, specially if high g's loads are considered.

8. Acknowledgements

This work was partially supported in part by the Fundação para a Ciência e Tecnologia (FCT) under Grant SFRH/BD/22861/2008 and project PTDC/EME-PME/64809/2006 and in part by the EU 7th Framework Project NOVEMOR.

9. References

[1] M. P. Bendsøe and N. Kikuchi. Generating optimal topologies in structural design using a homogenization method. *Computer Methods in Applied Mechanics and Engineering*, 71:197 – 224, 1988.

[2] G. Rozvany and M. Zhou. Application of the coc algorithm in layout optimization. *published in: Enginnering Optimization in Design Process, H.A. Eschenauer, C. Mattheck, N. Olhoff (Eds.)*, pages 59–77 (Proc. Int. Conf. held in Karlsruhe, Germany, Sept. 1990), 1991.

[3] L. Krog, A. Tucker, and G. Rollema. Application of topology, sizing and shape optimization methods to optimal design of aircraft components. In *3^{rd} Altair UK HyperWorks Users Conference*, 2002.

[4] K. Maute and G. W. Reich. An aeroelastic topology optimization approach for adaptive wing design. In *45^{th} AIAA/ASME/ASCE/AHS/ASC Structures, Structural Dynamics & Materials Conference*, Palm Springs, California, 19 - 22 April 2004.

[5] A. Gaspari and S. Ricci. Combining shape and structural optimization for the design of morphing airfoils. In *2^{nd} International Conference on Engineering Optimization*, Lisbon, Portugal, September 6 - 9 2010.

[6] A. A. Gomes and A. Suleman. Topology optimization of a reinforced wing box for enhanced roll maneuvers. *AIAA Journal*, 46(3):548–556, March 2008.

[7] Kai A. James and Joaquim R. R. A. Martins. Three-dimensional structural topology optimization of an aircraft wing using level set methods. In *Proceedings of the 12^{th} AIAA/ISSMO Multidisciplinary Analysis and Optimization Conference*, Victoria, BC, September 2008.

[8] Luis Félix, A. A. Gomes, and Afzal Suleman. Integration of strucutural topology optimization in a mdo framework. In *14^{th} AIAA/ISSMO Multidisciplinary Analysis and Optimization Conference*, Indianapolis, USA, Setember 2012.

[9] M. Bruyneel and P. Duysinx. Note on topology optimization of continuum structures including self-weight. *Structural Multidisciplinary Optimization*, 29:245–256, 2005.

[10] M. P. Bendsøe and O. Sigmund. *Topology Optimization: Theory, Methods and Applications*. Springer-Verlag, Berlin, 2003.

[11] Ole Sigmund. Morphology-based black and white filters for topology optimization. *Structural Multidisciplinary Optimization*, 33:401–424, 2007.

[12] O. Sigmund and J. Petersson. Numerical instabilities in topology optimization: a survey on procedures dealing with checkerboards, mesh-dependencies and local minima. *Structural Optimization*, 16:68–75, 1998.

[13] J. K. Guest, J. H. Prévost, and T. Belytschko. Achieving minimum length scale in topology optimization using nodal design variables and projection functions. *International Journal for Numerical Methods in Eng*, 61:238–254, 2004.

[14] K. Svanberg. A class of globally convergent optimization methods based on conservative convex separable approximations. *SIAM Journal of Optimization*, 12(2):555–573, 2002.